*Progress In Electromagnetics Research, PIER 72, 269–278, 2007*

# RELATIVE POWER DISTRIBUTIONS IN OMNIGUIDING PHOTONIC BAND-GAP FIBERS

**A.-B. M. A. Ibrahim**

School of Physics
Universiti Sains Malaysia
11800, Penang, Malaysia

**P. K. Choudhury**

Faculty of Engineering
Multimedia University
63100 Cyberjaya, Selangor, Malaysia

**Abstract**—Using Bloch formulations, an analysis is presented of the confinement of power in omniguiding photonic band-gap fibers of different dimensional values. Results are compared for four-layer and eight-layer fibers. Power peaks are observed that correspond to different propagation modes. Power patterns are found to be fairly smoothly matched at the different layer interfaces, which confirm the validity of the analytical approach.

## 1. INTRODUCTION

In 1987, Yablonovitch introduced the analogy between propagation of photons in dielectric mediums and propagation of electrons in semiconductors [1]. This ultimately gave birth to photonic band-gap materials and photonic crystal fibers, where a periodic variation in the RI is introduced, and the band-gap is formed for a certain range of photon energies [2]. Such band-gap materials are now of great interest owing to their multifarious potential applications in photonics [3–6].

Authors have reported earlier the useful characteristics of band-gap fibers for spectral filtering [6]. They also reported the dispersion characteristics [6] as well as the field patterns [7] of such fibers. Band-gap materials are usually multilayered mediums [8] which have potential applications in the area of integrated optics [9]. Some of the applications would be optical switching [4], Bragg-reflectors [5],

filtering [10–12] etc. Modal characteristics of multilayered and other waveguides have been presented before by Choudhury et al. [13–16]. Multilayered waveguides in the form of annular core cross-sections were also studied by Choudhury et al. [17–19] and Kumar et al. [20]. In these papers they did not consider the band-gap phenomenon. Yariv and Yeh [10] discussed the case of multilayered waveguides in analogy with the motion of electrons in periodic lattice structures. In the present paper too, we implement the quantum theory of electrons in solids, and demonstrate the confinement of power in band-gap fibers. We considered the cases when the two different types of layers are having the same as well as different values of thickness. The distribution of relative power is discussed for the cases of four-layer and eight-layer fibers. However, the field and power patterns in the case of band-gap fibers have been presented earlier by the authors [7], the present paper describes the relative power distributions in the different fiber layers.

## 2. THEORY

The refractive index (RI) profile of band-gap fiber under consideration is shown in Fig. 1, where $n_h$ and $n_l$ represent the RI values of the regions of two different types of layers; the region of RI $n_h$ ($n_h > n_l$) is having thickness $a$, and that of RI $n_l$ has $b$. We assume the high- and low-index mediums have the permittivity values as $\varepsilon_h$ and $\varepsilon_l$, respectively. Also, the mediums are non-magnetic in nature, i.e., the permeability $\mu \cong \mu_0$, the free space permeability. As the figure represents, there is a step-change in the RI values, and the fiber has periodicities in both RI as well as thickness. If $\psi = \psi\,(R, \phi, z, t)$ is the wave function, which is harmonic in time $t$ and coordinate $z$, the wave equation for the system of Fig. 1 will assume the form as

$$\frac{d^2\psi_R}{dR^2} + \frac{1}{R}\frac{d\psi_R}{dR} + \left\{\frac{\omega^2 n^2(R)}{c^2} - \beta^2 - \frac{v^2}{R^2}\right\}\psi_R = 0 \qquad (1)$$

where $\psi_R$ is the radial field component, $n(R)$ is the radial variation of RI, $\beta$ is the propagation constant, $\omega$ is the angular frequency, and

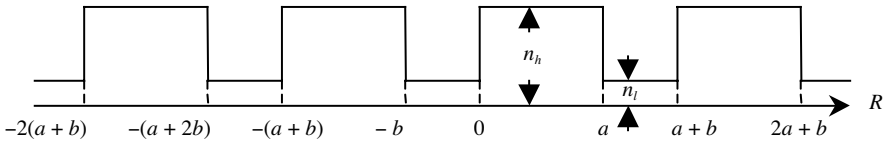


**Figure 1.** The profile of photonic band-gap fiber.

$v$ is the integer that represents the azimuthal periodicity. If the field has the form of Bloch waves, one can finally get the following set of differential equations [6] for the mediums of high and low RI values:

$$\frac{d^2U_h}{dR^2} + \left(\alpha_h - \beta^2\right) U_h(R) = 0 \quad \text{for} \quad 0 \le R \le a \tag{2a}$$

$$\frac{d^2U_l}{dR^2} + \left(\beta^2 - \alpha_l\right) U_l(R) = 0 \quad \text{for} \quad (a+b) \ge R \ge a \tag{2b}$$

where $\alpha_h \approx \left(\frac{\omega}{c}\right)^2 n_h^2$ and $\alpha_l \approx \left(\frac{\omega}{c}\right)^2 n_l^2$ with $U(R)$ as the Bloch function and $c$ as the speed of light. $U(R)$ will have the form as

$$U(R) = e^{jkr} u_k(R) \tag{3}$$

with

$$u_k(R) = u_k(R + a + b) \tag{4}$$

where $k$ is a real quantity. If the solutions of Eqs. (2a) and (2b) are matched at the layer boundaries, one may get the final eigenvalue equation [6] for the photonic band-gap fiber under consideration. Now the electric field can be represented as

$$E_z = \frac{1}{R^{1/2}} \left[C_1 e^{j\xi_h R} + C_2 e^{-j\xi_h R}\right] e^{j\beta z} e^{jv\phi} \quad \text{for} \quad 0 \le R \le a \tag{5}$$

and

$$E_z = \frac{1}{R^{1/2}} \left[C_3 e^{j\xi_l R} + C_4 e^{-j\xi_l R}\right] e^{j\beta z} e^{jv\phi} \quad \text{for} \quad (a+b) \ge R \ge a \tag{6}$$

with

$$\xi_h = (\alpha_h - \beta^2)^{1/2} \quad \text{and} \quad \xi_l = (\beta^2 - \alpha_l)^{1/2} \tag{7}$$

Further, in eqs. (5) and (6) $C_1, C_2, C_3$ and $C_4$ are the arbitrary constants to be determined by using the boundary conditions. This finally yields the values of constants $C_1, C_2$ and $C_4$ as

$$C_1 = C_3 \frac{2j\xi_l}{(j\xi_l + \xi_h)e^{a\xi_h}} \left[e^{jb\xi_l} e^{jkL} - \left\{\frac{e^{jb\xi_l} e^{jkL} - e^{a\xi_h}}{1 - e^{2a\xi_h}}\right\}\right] \tag{8a}$$

$$C_2 = C_3 \frac{2j\xi_l}{(j\xi_l - \xi_h)} \left[\frac{e^{jb\xi_l} e^{jkL} - e^{a\xi_h}}{e^{-a\xi_h} - e^{a\xi_h}}\right] \tag{8b}$$

$$C_4 = 2C_3 j\xi_l \left[\frac{1}{(j\xi_l + \xi_h)e^{a\xi_h}} \left\{e^{jb\xi_l} e^{jkL} - \left(\frac{e^{jb\xi_l} e^{jkL} - e^{a\xi_h}}{1 - e^{2a\xi_h}}\right)\right\} + \left\{\frac{e^{jb\xi_l} e^{jkL} - e^{a\xi_h}}{(j\xi_l - \xi_h)(e^{-a\xi_h} - e^{a\xi_h})}\right\} - \frac{1}{2j\xi_l}\right] \tag{8c}$$

In eqs. (9), $L = a+b$, and the values of the constants $C_1, C_2$ and $C_4$ are evaluated in terms of the constant $C_3$, which may be determined by a normalization condition taking into consideration the input power.

Using eqs. (5) and (6), the radial ($R$-) and the angular ($\phi$-) components of the electric/magnetic fields can be derived for the high-index as well as low-index regions of the omniguiding fiber. These field components are not incorporated into the text. Using those field components, and implementing the boundary conditions, the optical power [21] transmitted through the different fiber sections can be evaluated. If we represent the magnitude of power in the high- and low-index regions as $p_h$ and $p_l$, respectively, then the values of $p_h$ and $p_l$ will be

$$\begin{aligned} p_h \;=\; & \frac{1}{2}\left|\mathrm{Re}\int_0^{2\pi}\int_0^{R}\left[\left\{\frac{1}{R}\left(C_1e^{j\xi_hR}+C_2e^{-j\xi_hR}\right)\left[v\sin(v\phi)+\frac{1}{2}\cos(v\phi)\right]\right.\right. \\ & \left.-j\xi_h\left(C_1e^{j\xi_hR}-C_2e^{-j\xi_hR}\right)\cos(v\phi)\right\}e^{j\beta Z} \\ & \times\left\{\frac{j}{\xi_h^2}\frac{\beta}{\sqrt{R}}\left\{\frac{1}{R}\left(C_1e^{j\xi_hR}+C_2e^{j\xi_hR}\right)\left[v\sin(v\phi)-\frac{1}{2}\cos(v\phi)\right]\right.\right. \\ & \left.\left.+j\xi_h\left(C_1e^{j\xi_hR}-C_2e^{j\xi_hR}\right)\cos(v\phi)\right\}\right\}^{*}e^{-j\beta Z} \\ & -\left\{\frac{j}{\xi_h^2}\frac{\beta}{\sqrt{R}}\left\{\frac{1}{R}\left(C_1e^{j\xi_hR}+C_2e^{-j\xi_hR}\right)\left[v\sin(v\phi)-\frac{1}{2}\cos(v\phi)\right]\right.\right. \\ & \left.\left.+j\xi_h\left(C_1e^{j\xi_hR}-C_2e^{-j\xi_hR}\right)\cos(v\phi)\right\}e^{j\beta Z}\right\} \\ & \times\left\{-\frac{j}{\xi_h^2}\frac{1}{\sqrt{R}}\left\{\frac{1}{R}\left(C_1e^{j\xi_hR}+C_2e^{-j\xi_hR}\right)\right.\right. \\ & \times\left[\frac{1}{2}\frac{\beta^2}{\omega\mu_0}\cos(v\phi)-v\omega\varepsilon_h\sin(v\phi)\right] \\ & \left.\left.-\frac{j\beta^2\xi_h}{\omega\mu_0}\left(C_1e^{j\xi_hR}-C_2e^{-j\xi_hR}\right)\cos(v\phi)\right\}\right\}^{*}e^{-j\beta Z}\Bigg]RdRd\phi\Bigg| \end{aligned} \tag{9a}$$

$$p_l \;=\; \frac{1}{2}\left|\mathrm{Re}\int_0^{2\pi}\int_0^{R}\left[\left\{\frac{j}{\xi_l^2}\frac{\beta}{\sqrt{R}}\left\{\frac{1}{R}\left(C_3e^{j\xi_lR}+C_4e^{-j\xi_lR}\right)\right.\right.\right.$$

$$\times \left[ v\sin(v\phi) + \frac{1}{2}\cos(v\phi) \right] - j\xi_l \left( C_3 e^{j\xi_l R} - C_4 e^{-j\xi_l R} \right) \cos(v\phi) \Bigg\} e^{j\beta Z}$$
$$\times \left\{ \frac{j}{\xi_l^2} \frac{1}{\sqrt{R}} \left\{ -\frac{1}{R} \left( C_3 e^{j\xi_l R} + C_4 e^{-j\xi_l R} \right) \right.\right.$$
$$\times \left[ \frac{v\beta^2}{\omega\mu_0} \sin(v\phi) + \frac{\omega\varepsilon_l}{2} \cos(v\phi) \right]$$
$$\left.\left. + j\xi_l \omega\varepsilon_l \left( C_3 e^{j\xi_l R} - C_4 e^{-j\xi_l R} \right) \cos(v\phi) \right\} \right\}^* e^{-j\beta Z}$$
$$- \left\{ \frac{j}{\xi_l^2} \frac{\beta}{\sqrt{R}} \left\{ \frac{1}{R} \left( C_3 e^{j\xi_l R} + C_4 e^{-j\xi_l R} \right) \left[ v\sin(v\phi) - \frac{1}{2}\cos(v\phi) \right] \right.\right.$$
$$\left.\left. + j\xi_l \left( C_3 e^{j\xi_l R} - C_4 e^{-j\xi_l R} \right) \cos(v\phi) \right\} e^{j\beta Z} \right\}$$
$$\times \left\{ -\frac{j}{\xi_l^2} \frac{1}{\sqrt{R}} \left\{ \frac{1}{R} \left( C_3 e^{j\xi_l R} + C_4 e^{-j\xi_l R} \right) \right.\right.$$
$$\times \left[ \frac{1}{2} \frac{\beta^2}{\omega\mu_0} \cos(v\phi) - v\omega\varepsilon_h \sin(v\phi) \right]$$
$$\left.\left. - \frac{j\beta^2\xi_l}{\omega\mu_0} \left( C_3 e^{j\xi_l R} - C_4 e^{-j\xi_l R} \right) \cos(v\phi) \right\} \right\}^* e^{-j\beta Z} \Bigg] RdRd\phi \Bigg| \tag{9b}$$

In eqs. (9), the values of constants $C_1, C_2, C_3$ and $C_4$ are as defined in eqs. (8). As mentioned above, the constant $C_3$ can be determined by a normalization condition taking into consideration the input power. If $p_t$ represents the total power transmitted through the omniguiding fiber, then $p_h/p_t$ and $p_l/p_t$ will, respectively, represent the relative power (or the confinement factor) in the high-index and the low-index regions of the fiber.

## 3. RESULTS AND DISCUSSION

Figures 2–4 show the variation of the theoretically estimated values of the relative power distributions in the guiding and the non-guiding regions (of the omniguiding Bragg fiber) against the radial distance. Different number of fiber layers have been taken into account, e.g., in our illustrative cases, we considered four- and eight-layers, in order to see the effect of the number of layers on the transmission of power. In order to plot all these graphs, the operating wavelength is kept fixed

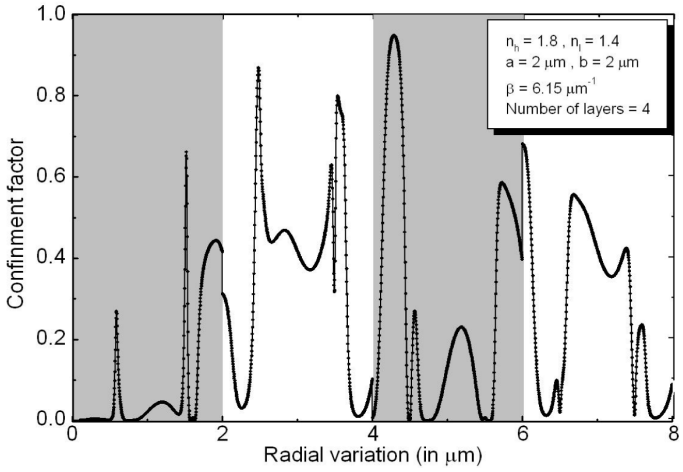


**Figure 2.** Plot of confinement factor for four-layer fiber with $a = b = 2\,\mu$m.

at $1.55\,\mu$m. This is because of the advanced interest being paid by the present R&D community toward the development of low cost in-line fiber components suitably working at $1.55\,\mu$m. Further, fibers offer low loss at $1.55\,\mu$m window. As the width of the section is fixed, these plots show how the power is distributed over the number of modes sustained for a fixed value of azimuthal mode index. (In our analytical treatment, however, we considered relatively lower order modes). This is why we observe several peaks in these graphs corresponding to certain values of the radial distance. These peaks, therefore, represent the various modes sustained in the fiber. At this point, this is to be mentioned that a study of such omniguiding Bragg fibers has been reported earlier by the authors, in which they presented the plot of eigenvalue equation for the system [6], and the variation of fields in the different fiber sections [7]. The dispersion characteristics of such fibers were also investigated [6], and the band-gap features were reported. It was found that the number of allowed bands increases with the index difference between different layers, and also, the allowed bandwidth becomes higher in the cases corresponding to larger thickness values. Further, it was found that, by using Bloch formulation, the analytical treatment leads to the smooth match of fields in different fiber sections, which confirms the validity of the implementation of the quantum theory of electrons.

Figure 2 corresponds to the case when both the layers are of the same thickness, viz. $2\,\mu$m. In this illustrative case, four layers are considered, and the low- and the high-index regions have RI values as

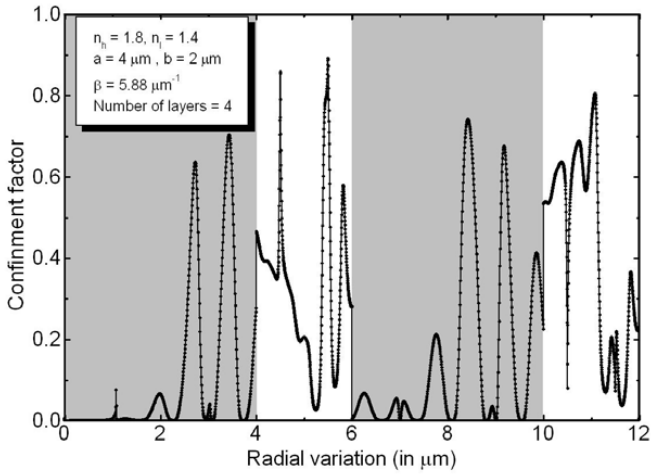


**Figure 3.** Plot of confinement factor for four-layer fiber with $a = 4\,\mu$m and $b = 2\,\mu$m.

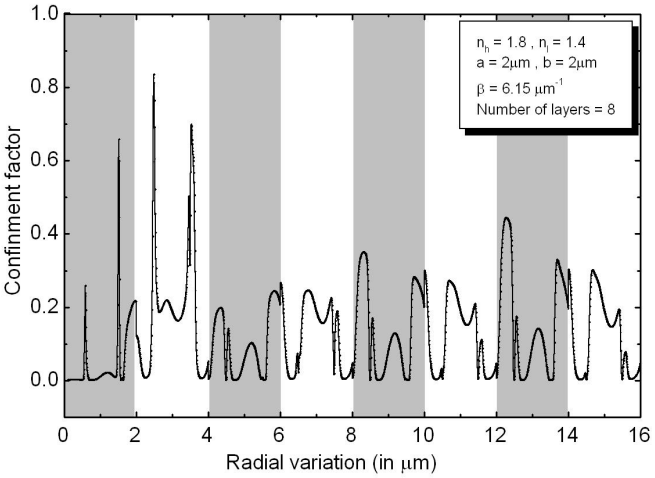


**Figure 4.** Plot of confinement factor for eight-layer fiber with $a = b = 2\,\mu$m.

1.4 and 1.8, respectively. The allowed value of $\beta$ in the intermediate region is taken to be $6.15\,\mu\mathrm{m}^{-1}$. We observe the existence of several peaks in the graph, which essentially represent various modes sustained by the guide. Also, we find that, like the fields [7] in different sections of the fiber, the relative power distributions too match almost smoothly at different layer boundaries.

With the same RI values and the same number of layers, when the high-index layer thickness is doubled (Fig. 3), number of peaks within the structure is also almost doubled, indicating thereby a proliferation in the number of existing modes. This is as expected because more number of modes can be sustained in waveguides with higher dimensions. In this case too, the allowed intermediate value of the propagation constant is taken to be $6.15\,\mu\mathrm{m}^{-1}$.

We further observe the case when the number of layers is just doubled, viz. eight (Fig. 4). The rest of the parameters are kept the same, i.e., $n_h = 1.8$, $n_l = 1.4$ and $\beta = 6.15\,\mu\mathrm{m}^{-1}$. The layer thicknesses are also kept the same, viz. $a = b = 2\,\mu\mathrm{m}$. We see that the number of sustained modes is much more enhanced in this case, which is evident from the higher number of power peaks in this case. We generally observe that, with the increase in radial distance, the confinement factor generally decreases. Further, we observe the common feature in all the cases that the confinement factors in the different fiber sections match in a fairly smooth way, which essentially confirms the validity of our analytical approach.

## 4. CONCLUSIONS

From the foregoing analysis, conclusions can be drawn that more number of propagation modes exist in the fiber when the thickness of the high-index layer is increased. Power peaks demonstrate the existence of different modes in the fiber. The confinement factor reduces with the increase in radial distance. A fairly smooth match of power in the different sections confirms our analysis (based on fairly simpler quantum theory of electrons) to be valid.

## ACKNOWLEDGMENT

This paper is dedicated to the great scientist Prof. Roger A. Lessard whose recent demise is a tragic loss to the international optics community. He was the Director of the Department of Physics, Engineering Physics and Optics and the Founder Director of the Centre for Optics, Photonics and Lasers (COPL) at Université Laval (Quebec, Canada). His dedication to the development of optics in Quebec and

internationally cannot be forgotten. One of the authors (PKC) was blessed to work with this widely beloved gentleman.

## REFERENCES


1. Yablonovitch, E., "Inhibited spontaneous emission in solid-state physics and electronics," *Phys. Rev. Lett.*, Vol. 58, 2059–2062, 1987.
2. Guenneu, S., A. Nicolet, F. Zolla, and S. Lasquellec, "Numerical and theoretical study of photonic crystal fibers," *Progress In Electromagnetics Research*, PIER 41, 271–305, 2003.
3. Fan, S., P. Villeneuve, and J. D. Joannopouls, "Large omnidirectional bandgaps in metalodielectric photonic crystals," *Phys. Rev. B*, Vol. 54, 11245–11251, 1996.
4. Villeneuve, P., D. Abrams, S. Fan, and J. D. Joannopouls, "Single-mode waveguide microcavity for fast optical switching," *Opt. Lett.*, Vol. 21, 2017–2019, 1996.
5. Fink, Y., J. Winn, S. Fan, C. Chen, J. Michel, J. D. Joannopouls, and E. Thomas, "A dielectric omnidirectional reflector," *Science*, Vol. 282, 1679–1682, 1998.
6. Ibrahim, A.-B. M. A., P. K. Choudhury, and M. S. B. Alias, "Analytical design of photonic band-gap fibers and their dispersion characteristics," *Optik*, Vol. 116, 169–174, 2005.
7. Ibrahim, A.-B. M. A., P. K. Choudhury, and M. S. B. Alias, "On the analytical investigation of fields and power patterns in coaxial omniguiding Bragg fibers," *Optik*, Vol. 117, 33–39, 2006.
8. Wu, C.-J., "Transmission and reflection in a periodic superconductor/dielectric film multilayer structure," *J. Electromag. Waves and Appl.*, Vol. 19, 1991–1996, 2006.
9. Zheng, Q. R., Y. Q. Fu, and N. C. Yuan, "Characteristics of planar PBG structures with a cover layer," *J. Electromag. Waves and Appl.*, Vol. 20, 1439–1453, 2006.
10. Yeh, P., A. Yariv, and C. S. Hong, "Electromagnetic propagation in periodic stratified media — I. General theory," *J. Opt. Soc. Am.*, Vol. 67, 423–438, 1977.
11. Farries, M. C., J. E. Townsend, and S. B. Poole, "Very high-rejection optical fiber filter," *Electron. Lett.*, Vol. 22, 1126–1128, 1986.
12. Chen, J. C., A. Haus, S. Fan, P. Villeneuve, and J. D. Joannopouls, "Optical filters from photonic band-gap air bridges," *J. Light. Tech.*, Vol. 14, 2575–2580, 1996.

13. Choudhury, P. K., P. Khastgir, S. P. Ojha, and L. K. Singh, "Weak guidance in bent and unbent four layer planar waveguides," *Jpn. J. Appl. Phys.*, Vol. 31, L39–L42, 1992.
14. Choudhury, P. K., P. Khastgir, S. P. Ojha, and K. S. Ramesh, "An exact analytical treatment of parabolically deformed planar waveguides near cutoff," *Optik*, Vol. 95, 147–151, 1994.
15. Choudhury, P. K. and O. N. Singh, "Some multilayered and other unconventional lightguides," *Electromagnetic Fields in Unconventional Structures and Materials*, O. N. Singh and A. Lakhtakia (eds.), 289–357, Wiley, USA, 2000.
16. Lim, M. H., S. C. Yeow, P. K. Choudhury, and D. Kumar, "On the dispersion characteristics of tapered core dielectric optical fibers," *J. Electromag. Waves and Appl.*, Vol. 20, 1597–1609, 2006.
17. Choudhury, P. K. and R. A. Lessard, "An estimation of power transmission through a doubly clad optical fiber with annular core," *Microw. and Opt. Tech. Lett.*, Vol. 29, 402–405, 2001.
18. Choudhury, P. K., "Relative power distribution in an infrared annular core optical fiber," *Optik*, Vol. 112, 479–482, 2001.
19. Choudhury, P. K. and T. Yoshino, "A rigorous analysis of the power distribution in plastic clad annular core optical fibers," *Optik*, Vol. 113, 481–488, 2002.
20. Kumar, D. and O. N. Singh II, "Analysis of the propagation characteristics of a step-index waveguide of annular circular cross-section with conducting helical windings on the inner and outer boundary surfaces between the guiding and the non guiding regions," *J. Electromag. Waves and Appl.*, Vol. 18, 1655–1669, 2004.
21. Choudhury, P. K. and T. Yoshino, "TE and TM modes power transmission through liquid crystal optical fibers," *Optik*, Vol. 115, 49–56, 2004.